https://doi.org/10.3176/eco.2007.1.01
Proc. Estonian Acad. Sci. Biol. Ecol., 2007, **56**, 1, 5–18

Calibration of time series of satellite images to study the seasonal course of forest reflectance

Tiit Nilson[a,c*], Tõnu Lükk[a], Sandra Suviste[b], Heidi Kadarik[b], and Alo Eenmäe[c]

[a] Tartu Observatory, 61602 Tõravere, Tartumaa, Estonia; tonu.lukk@mail.ee
[b] Institute of Environmental Physics, University of Tartu, Ülikooli 18, 50090 Tartu, Estonia; sandras@ut.ee, heidikadarik@hot.ee
[c] Institute of Forestry and Rural Engineering, Estonian University of Life Sciences, Kreutzwaldi 5, 51014 Tartu, Estonia; alo@rrg.edu.ee

Received 27 January 2006, in revised form 16 June 2006

Abstract. A seasonal series of Landsat TM and SPOT images over a forest area at Järvselja, Estonia, was compiled from the set of images acquired in 1986–2003 to study the seasonal changes in reflectance among different forest types. All images were transformed into ground-level reflectance factor units and the seasonal courses of reflectance were constructed for several forest types in six reflective bands of Landsat TM. Different forest types were extracted by respective queries from the forestry database of Järvselja. The seasonal time course was presented as a function of temperature time. The calibration coefficients of all images in the series were corrected to obtain a smooth seasonal course of reflectance for fertile stands dominated by spruce, pine, and birch as dark targets, and *Pinus* bogs as bright targets. The smoothed seasonal series of reflectance are now suitable for a further quantitative analysis for the main driving factors.

Key words: remote sensing, seasonal course, forest types, Landsat TM, SPOT.

INTRODUCTION

Modern satellite remote sensing has many applications in different aspects of vegetation study. Among others it provides a possibility of investigating the seasonal course of vegetation. Monitoring seasonal changes is important in several problems, including the estimation of productivity of different vegetation types and the discrimination between these types. The medium and coarse resolution satellite systems, such as MODIS (Moderate Resolution Imaging Spectroradiometer),

* Corresponding author, nilson@aai.ee

produce almost continuous data over the whole Earth and thus the information on reflectance seasonal changes at a coarse scale and in large territories is relatively well represented. Nevertheless, there is surprisingly little quantitative information available about the seasonal course of reflectance of different forest and natural vegetation types produced by higher resolution satellite systems, such as Landsat and SPOT (Satellite Pour l'Observation de la Terra). Time series of finer resolution imagery enable us to study phenology-related seasonal changes of different forest types located in a rather limited territory. However, due to cloudiness conditions in the boreal and sub-boreal zones, it appears to be impossible to obtain a sufficient amount of images to form readily tractable seasonal series from one single year. As a result, we have to create the seasonal time series from images of several years.

A serious problem with the time series of satellite images is how to transform the images into comparable units. When Landsat-type images are concerned, a logical way is to transform all images into surface-level reflectance factor units. However, at the present quality level of sensor absolute calibration and of atmospheric correction of images needed for this transformation, the resulting time series typically appears to be rather scattered. The aim of the present paper is to show a possible way to obtain smoother time series more appropriate for interpretation. The main attention is paid to the seasonal reflectance curves of different forest types with the selection of forests made with the help of existing forestry databases.

MATERIALS AND METHODS

The forests under study with a total area of approximately 10 000 ha belong to the Järvselja Training and Experimental Centre at the Estonian University of Life Sciences. The study area is located on a low plain near Lake Peipsi in south-east Estonia (with a 'centre' located at 58°15′ N, 27°28′ E). The dominating tree species are birch (*Betula pendula*, *B. verrucosa*), Scots pine, and Norway spruce. The site types vary over a large range from fertile *Aegopodium*, *Oxalis*, and *Filipendula* types to unfertile transitional and raised bog, lowland mire, and *Vaccinium uliginosum* types. The forestry databases together with the digital maps of stand borders over the region used in this study originate from 1993/1994 and 2001.

In the present study, a time series of images containing 14 Landsat Thematic Mapper (TM) and 9 SPOT images over the Järvselja forested region was used. The satellite images were acquired in 1986–2003 at different moments of the growing season and enable us to study the seasonal changes in reflectance among different forest types represented at Järvselja. All the images were registered in the Estonian base map coordinate system using a set of control points. Although the spectral bands of Landsat and SPOT do not exactly coincide (see Table 1), the images in green (TM2 and XS1), red (TM3 and XS2), near infrared (NIR) (TM4 and XS3), and middle infrared (MIR) (TM5 and XS4) bands were treated as

belonging to the same band. As SPOT has no equivalent bands for Landsat TM bands TM1 and TM7, the time series contained less images in these bands. Some images (Table 2) of the time series are from the earlier versions of SPOT, which have no MIR band.

Table 1. The list of spectral bands used in forming the time series of images

Landsat TM band	Wavelengths, nm	SPOT band	Wavelengths, nm
TM1, blue	450–520		
TM2, green	520–600	XS1, green	500–590
TM3, red	630–690	XS2, red	610–680
TM4, NIR	780–900	XS3, NIR	780–890
TM5, MIR	1550–1750	XS4, MIR	1580–1750
TM7, MIR	2080–2350		

Table 2. The list of Landsat and SPOT images used to form the seasonal time series of images together with the temperature time and solar elevation

Year of acquisition	Day of year	Temperature time, degree day	Temperature time, average, degree day	Sun elevation, degrees	Scanner
1988	136	108	154	48.3	Landsat 5
1994	129	116	112	48.9	SPOT 3
1994	130	127	118	45.9	Landsat 5
2000	129	176	112	47.4	Landsat 7
1992	147	185	226	49.8	Landsat 5
1998	132	198	128	47.3	Landsat 5
1996	143	200	199	48.2	Landsat 5
2002	152	350	265	51.5	Landsat 7
2000	157	419	314	52.7	Landsat 7
2003	175	473	503	54.8	SPOT 4
2001	176	477	514	54.5	SPOT 2
1986	166	492	410	54.6	SPOT 1
1992	180	546	559	51.2	Landsat 5
2001	185	595	618	53.9	SPOT 4
1999	191	803	695	51.7	Landsat 7
2002	195	863	747	53.0	SPOT 4
1992	206	882	883	51.3	SPOT 1
2002	200	939	807	50.2	Landsat 7
1997	225	1057	1120	46.2	SPOT 1
2000	239	1258	1266	46.2	SPOT 4
1997	241	1276	1286	38.6	Landsat 5
1995	236	1290	1237	38.2	Landsat 5
2002	232	1405	1196	42.3	Landsat 7

Because of phenology differences between different years, the seasonal sequence of the images was constructed based rather on temperature (phenology) time than on date (day of year). Being defined as the sum of daily average temperatures exceeding 5 °C, temperature time proceeds faster during a warm period compared with a colder period of time. The temperature data used in this study are from Tartu Meteorological Station located at Tõravere (58°16′ N, 26°28′ E). The list of images used together with the temperature time is presented in Table 2. The temperature time is given for the day of image acquisition, and as the average over the years 1986–2003 for that day of year. By comparing two temperature time columns in Table 2, the reader can have an idea how far the temperature time was at the moment of image acquisition from the temperature time of an 'average' year.

The forest area under study partly reaches the adjacent large wetland (Great Fen of the Emajõgi River) in the north and often suffers from excessive moisture. Thus the vegetation development in the Järvselja area is influenced by the above-ground water level. The water level in Lake Peipsi as measured by the Estonian Meteorological Institute at Praaga, located at the estuary of the Emajõgi River, was used to describe water conditions at the moments of image acquisition.

All the images were atmospherically corrected using the radiative transfer package 6S (Vermote et al., 1997). For the latest satellite images the sun-photometer data from the Tõravere station of the NASA Aeronet network (http://aeronet.gsfc.nasa.gov, accessed 7 November 2005) were used to describe the atmospheric aerosol constituents and water content. For earlier images the sunphotometer data were not available. The subarctic-summer aerosol model was applied and the water content was estimated from the data of Tartu Meteorological Station. The ozone content data were retrieved from NASA's TOMS network (http://toms.gsfc.nasa.gov, accessed 7 November 2005). Using forest inventory databases, mid-age and older pure Norway spruce stands were selected from the test area. Their radiance values were measured from the satellite images to be used as 'dark' reference objects. The Kuusk–Nilson (2000) forest reflectance model was used to simulate the reflectance values for TM3/XS2 equivalent wavelength and particular type of forest for temperature times equal to those of satellite image acquisitions. Altering the aerosol optical thickness value, a set of 6S input parameters was fixed at a level that resulted in the test area reflectance equal to the simulated value. This set of parameters was subsequently used to calculate the calibration coefficients for the selected spectral bands of a satellite image.

This way linear relations between the digital numbers (DN) of the original image and ground level reflectance factors (R) were established by the relation

$$R_{ij} = DN_{ij} b_{ij} + a_{ij}, \tag{1}$$

where b_{ij} stands for the slope and a_{ij} for the intercept of the relation, the subscript i denotes the image and j the spectral band number.

Queries were made for information from the forestry database of Järvselja from 1993/1994 to select forests of specific type according to main tree species,

site type, and quality. Additional refinement in the queries was made so that the forest stands had to be at least 1 ha in size, the age of a stand should be between 30 and 60 years, and the stands must not have been cut during the period of interest (from 1986 to 2003). In all the queries the main tree species had to form at least 75% of the total basal area.

The queries from the database, the extraction of pixels, and the calculation of average reflectances for the forests in the query were made by the program PixelWin (Lükk, 1999). Stand area weighted average reflectances in DN units and further in reflectance factor units (Eq. 1) in all available spectral bands were calculated for each forest type.

The average reflectance factors of each queried forest type R_{ijk} were plotted against the temperature time, and smooth curves were drawn through the scatterplots using 4-order (or sometimes lower order) polynomials (e.g., Fig. 1). Then the residuals between the smoothed curve and initial reflectance values were calculated. A new slope and intercept were calculated for each band and image to minimize the squared sum of residuals over preselected forest types. From the least-square minimizing condition, we find

$$b_{ij} = \frac{\sum_{k=1}^{n} DN_{ijk} R_{ijk}^{sm} - \frac{1}{n}\sum_{k=1}^{n} DN_{ijk} \sum_{k=1}^{n} R_{ijk}^{sm}}{\sum_{k=1}^{n} DN_{ijk}^2 - \frac{1}{n}\left(\sum_{k=1}^{n} DN_{ijk}\right)^2},$$

$$a_{ij} = \sum_{k=1}^{n} R_{ijk}^{sm} - \frac{b_{ij}}{n}\sum_{k=1}^{n} DN_{ijk} \qquad (2)$$

for the corrected slope and intercept, respectively. Here, subscript k $(k = 1, 2, \ldots, n)$ stands for the preselected forest type, and R_{ijk}^{sm} denotes the smoothed value of the reflectance for forest class k, image i, and band j as calculated from the polynomial (or other type) approximation of initial reflectances; DN_{ijk} is the average reflectance of forest type k from image i and band j in the original DN units.

In this particular study, the following four $(n = 4)$ forest types were chosen for correcting the slope and intercept values by relation (2):

- spruce forests (they are all growing on fertile sites), altogether 57.3 ha;
- pine forests growing on fertile sites (Orlov (1929) site index <3), 50.2 ha;
- birch forests growing on fertile sites (Orlov site index <3), 121.9 ha;
- *Pinus* bogs, 436 ha.

Forests on fertile sites were chosen for smoothing because their seasonal development should not be too much influenced by factors other than the sum of daily temperatures. As all the fertile site forests are relatively dark, we need a brighter target to obtain reliable estimates of slope and intercept in Eq. 2. As a bright target, *Pinus* bog was chosen. First of all, we have a considerable amount of *Pinus* bogs in the region. Bogs are known as unique change-resistant eco-

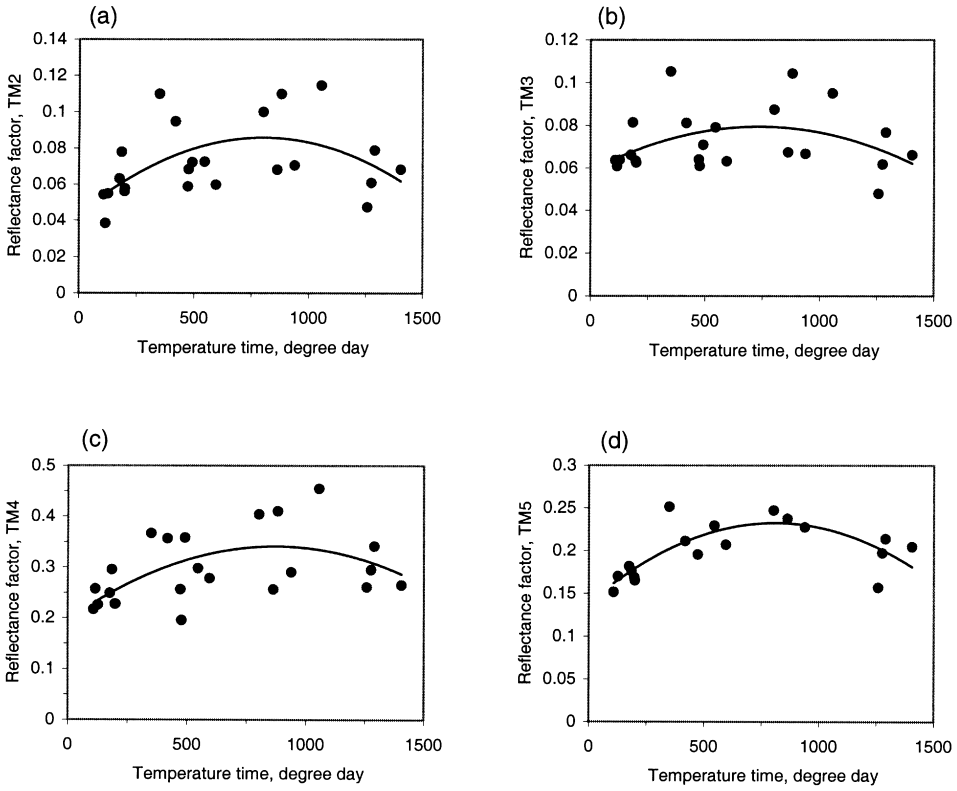

Fig. 1. Seasonal course of reflectance of the *Pinus* bog from Järvselja as determined from non-smoothed time series of the images. Four spectral bands corresponding to Landsat TM bands: (a) – TM2 (green), (b) – TM3 (red), (c) – TM4 (near infrared), and (d) – TM5 (middle infrared).

systems with a minimum seasonal course. Moreover, the life cycle of bogs is practically not influenced by the water level in adjacent lakes like great Lake Peipsi, which is important in our case. The problem with *Pinus* bogs is that their reflectance depends on the sun angle.

After estimating new slope and intercept values of the *DN*–reflectance relation, reflectance factors were recalculated for all images and all spectral bands. As a result, corrected seasonal time series of all the selected forest types were obtained.

In addition to the four forest types used to smooth the time series, the following forest types were considered in this paper:

– black alder forests growing on fertile sites, 51.5 ha;
– pine forests growing on infertile sites (Orlov site index >3), 25.3 ha;
– birch forests growing on infertile sites (Orlov site index >3), 311.9 ha;
– birch forests growing on a lowland mire, 1587 ha;
– treeless lowland mire, 37.5 ha.

The range of stand data among the selected forests is given in Table 3.

Table 3. The range of stand inventory data among the forests selected for the analysis

	Spruce	Fertile pine	Infertile pine	Fertile birch	Infertile birch	Black alder	*Pinus* bog
Dominating species	Spruce	Pine	Pine	Birch	Birch	Black alder	Pine
Age, years	31–55	36–57	32–50	35–45	35–45	35–55	–
Tree height, m	10–22	13–23	6–10	14–22	7–13	15–25	–
Trunk diameter, cm	12–22	14–25	9–14	11–19	8–12	14–25	–
Volume (m^3/ha)	105–332	171–316	53–87	111–255	37–138	163–367	–
Basal area (m^2/ha)	17–35	24–33	14–18	14–29	8–22	23–34	–
Stem number (trees/ha)	631–2210	602–1867	1039–2292	696–2210	796–2387	611–2079	–
Stock density	7–12	7–12	6–8	6–11	5–10	8–12	1–7
Site index (Orlov)	1a–3	1a–2	4–5	1–2	4–5	1–2	5–5a

– Not measured.

RESULTS

After correcting the slope and intercept values of all images in the time series, the seasonal changes of reflectance among the selected four forest types became much smoother (see Figs 2 and 3) than before. It should be noted that, as a result of smoothing, some changes appear in the shape of the new smoothed curve as well.

Comparison of the seasonal reflectance courses in three Scots pine dominated forest types of very different fertility (Fig. 2) shows that the community growing on the poorest site is the brightest in all bands and the most fertile community is the darkest. This fact agrees well with the Monteith (1972) hypothesis, at least when the visible bands TM1, TM2, and TM3 are concerned. As revealed by the ground-based radiometric measurements, in agricultural crops and grass communities (e.g., Nilson, 1988; Peterson, 1992) a minimum reflectance at the peak of growing season is present in the red band due to the pronounced chlorophyll absorption. However, the apparent seasonal curve in the red band of the *Pinus* bog is bell-shaped with a maximum in the middle of the season while that of the fertile pine is almost constant. To explain this phenomenon, one has to remember that in such a seasonal time series of images, a seasonal course of the sun angle is present (see Table 2). From model simulation (Kuusk & Nilson, 2000) we expect that the higher the sun, the higher should be the forest reflectance in the nadir view direction. So, if there were no changes in the stand structural and optical parameters, all forests should have at least a slightly bell-shaped seasonal course due to the seasonal change in the sun angle. Preliminary simulations

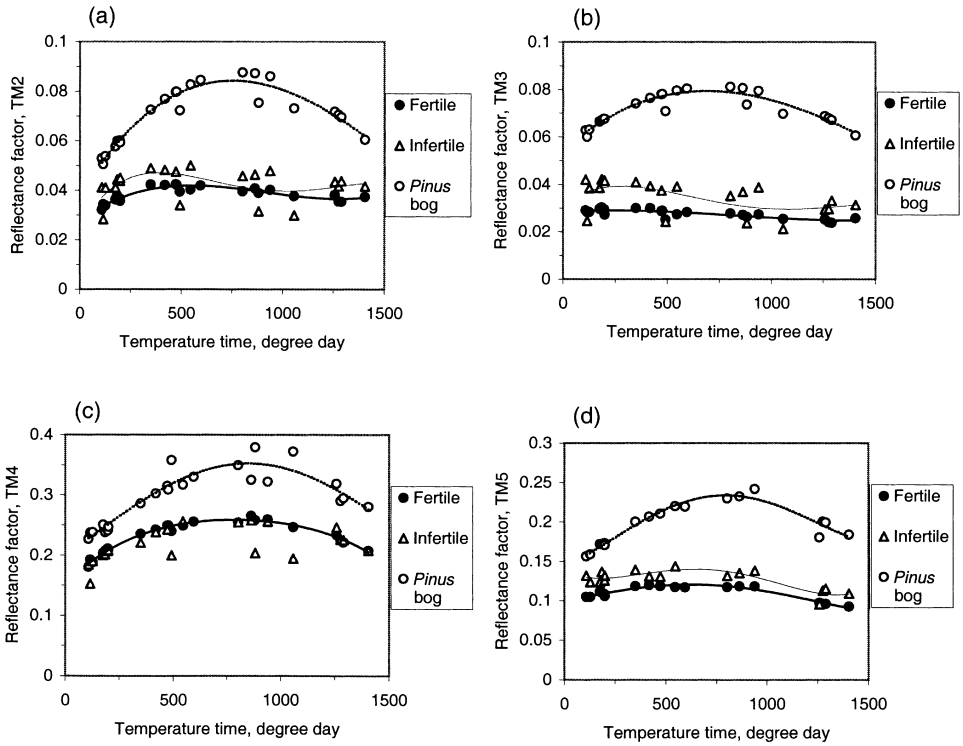

Fig. 2. Smoothed seasonal courses of different pine dominated forests from Järvselja: fertile and infertile pine and *Pinus* bog. Spectral bands as in Fig. 1.

showed that the only exception in that could be the near infrared band where a rather insensitive or sometimes the opposite behaviour was found. Evidently, we do not see the bell-shaped curve of fertile pine stands in TM3 as there is some increase in the photosynthesizing biomass and the amount of chlorophyll per unit ground area in the middle of the growing season. As for the *Pinus* bog with a relatively sparse tree canopy, the simulations predict a higher sensitivity of reflectance with respect to the change in the sun angle than in denser stands. In the *Pinus* bog, only moderate seasonal changes occur in the photosynthesizing needle area of the tree layer and the leaf area of the ground vegetation. In the near infrared band TM4, the fertile and infertile pine forests have a quite similar seasonal course, both in the size and the shape of the curve. These facts should be verified by further model simulations, i.e. by applying forest reflectance models (Kuusk & Nilson, 2000; Nilson et al., 2003).

When the proposed method of smoothing is applied, the seasonal courses of reflectance for the average forests in each of the selected forest type become more or less smooth. Naturally, the larger the acreage of the selected forest type, the

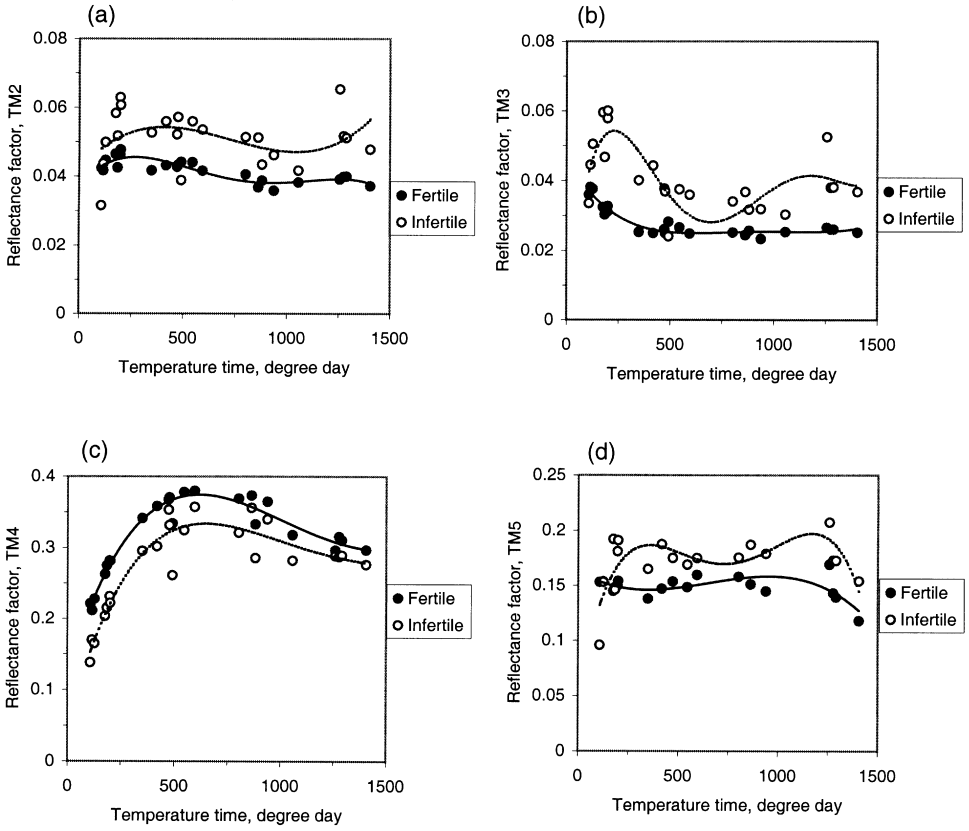

Fig. 3. Seasonal course of reflectance for fertile and infertile birch dominated forests from Järvselja. Spectral bands as in Fig. 1.

smoother the result will be. Similarly, we can now follow the seasonal reflectance courses of individual stands. However, more or less stable time series for individual forest stands can be expected if the stands are sufficiently large to minimize the effect of mixed border pixels, adjacency effects, and uncertainties introduced by image rectification. A rough practical estimate from our present study is that for Landsat and SPOT image series a stand should be at least 5 ha in area to guarantee a more or less smooth seasonal sequence of reflectance.

When comparing the seasonal reflectance courses in fertile and infertile birch stands (Fig. 3), the infertile stands appear to be more reflective than the fertile stands in all TM bands, except for the near infrared band TM4. In that sense, the birch stands act more like herbaceous vegetation. However, specific differences in the shape of seasonal reflectance curves between fertile and infertile birch stands can be noticed, too. Especially in the early spring there are qualitatively different

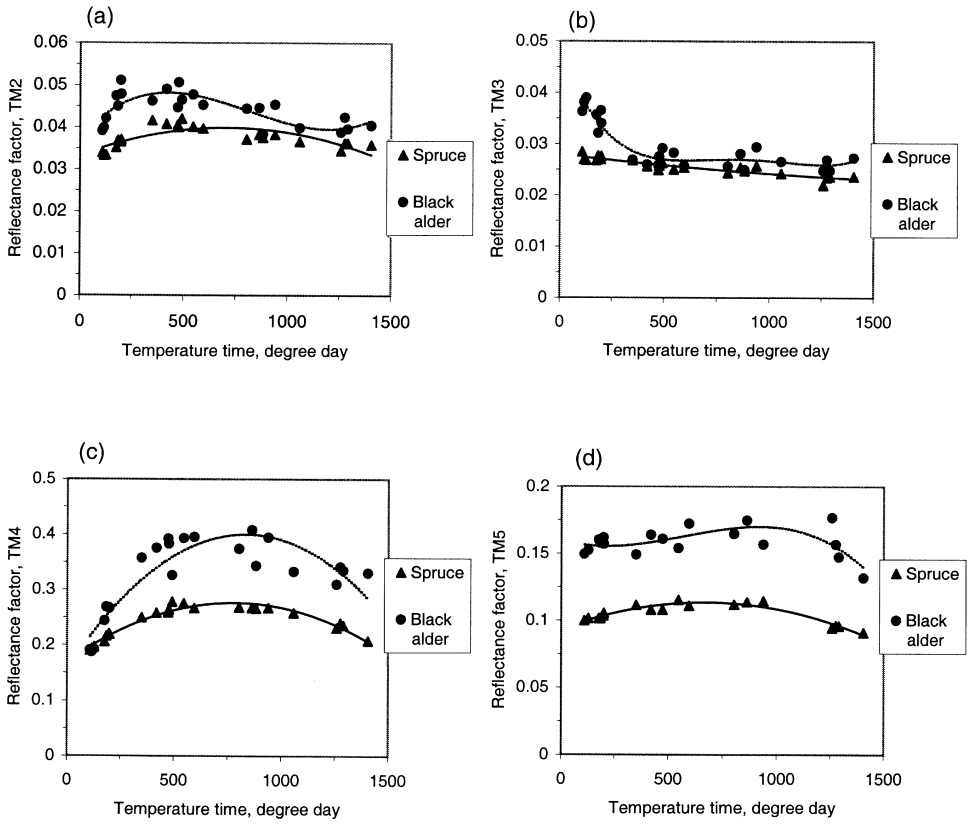

Fig. 4. Seasonal course of reflectance in four spectral bands for spruce and black alder dominated forests as determined from the smoothed time series. Spectral bands as in Fig. 1.

reflectance courses, the green development in the infertile stands starts later and at first the soil seems to start to dry in spring before the onset of green development in the understorey and the tree layer. From the reflectance curves, no such separate period of drying could be noticed in the fertile birch stands, i.e. drying of soil and green development proceed simultaneously.

The seasonal reflectance curves of spruce and black alder dominated stands are compared in Fig. 4. These two types of forest can be discriminated from each other in bands TM4 and TM5 during the whole season. In bands TM2 and TM3 the reflectance differences appear only in early spring.

Figure 5 presents the seasonal courses of reflectance in the same four bands for the treeless lowland mire. The points on the graph are discriminated into high and low water level by the water level in Lake Peipsi. We see that there are systematic differences between the lowland mire reflectances measured in wet

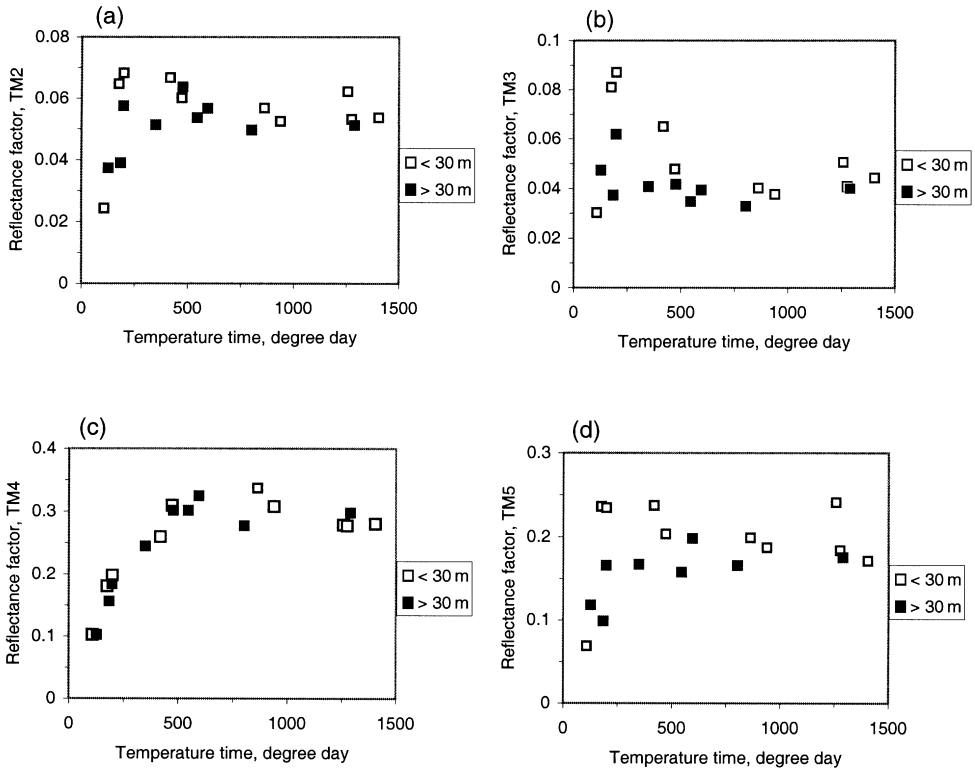

Fig. 5. Seasonal course of reflectance of a treeless lowland mire in wet (water level at Praaga >30 m) and dry (<30 m) years. Spectral bands as in Fig. 1.

and dry years. This kind of dual temporal signature could even be used to discriminate the vegetation types subject to flooding from other types.

It is not easy to explain why there is practically no difference between the wet and dry years in the near infrared band TM4. A similar situation was found when we analysed the data for the birch lowland mire (results not given here). If in wet years the water level in lowland mires is so high that some water surface is exposed through the vegetation, then the effect of the presence of the water surface should lead to the diminishing of reflectance in all spectral bands considered. Only if the coverage of green vegetation is higher in wet years, these two effects could more or less compensate each other in band TM4, while in other bands both the increased cover and higher water surface contribution have a diminishing effect on reflectance. However, presently we have no evidence that the green vegetation cover of the lowland mire was higher in wet years than in dry years.

From smoothing, seasonal courses of acceptable quality were obtained for bands TM1 (blue) and TM7 (middle infrared), too (not presented here). The smoothing improved the results especially in band TM1, which is strongly influenced by variable atmospheric conditions.

DISCUSSION

The smoothing of calibration constants of time series of Landsat and SPOT images appears to be possible, because the reflectance variations among different forest types are largely consistent. However, some variations still remain and some images for some forest classes fall out also of the smoothed series.

The justification for the smoothing procedure applied remains somewhat problematic. Certainly, the temperature time used to level out the phenology differences between different years cannot account for all environmental differences. However, as a first approximation, creating the time series based on temperature time seems to be a good option. Nevertheless, we are aware that some of the systematic differences between years could be levelled out as a result of the smoothing applied. For instance, the water content in the understorey moss can be rather different in dry and wet years. However, the main goal of obtaining smooth seasonal reflectance series is just a possibility of comparing these to the simulated seasonal curves for an 'average' year.

To some extent, the final result will depend on the forest classes chosen for smoothing the time series and on the type of smoothing curve. Alternatively to the polynomial approximation, other types of smoothing curves, like the cubic spline, could be used.

The reader should note that among the forest types selected for smoothing at least one should be dark and one relatively bright, then the slope and intercept of relation (1) could be more reliably found. Ideally, these chosen forest classes should have a constant reflectance throughout the season.

The number and selection of the control types of vegetation could easily be changed, weights could be given to different classes, e.g. according to the acreage of each class. When we omitted one or two forest types from smoothing (keeping the *Pinus* bog as one) the results did change somewhat, but not too much.

One of the important factors in such reflectance seasonal series is the course of the sun's elevation. If the studied vegetation type shows a dependence of reflectance on the sun angle, the time series had a clear seasonal course even if there were no phenological changes in the vegetation. The reason is that the sun angle at the time of image acquisition changes along with the date (see Table 2). This fact could (at least partly) explain why some of the SPOT images are outliers with respect to dominating in the series Landsat images even in the smoothed time series. The SPOT images are acquired somewhat later in daytime and closer to noon and with a higher sun if compared with the neighbouring in time Landsat images. With the higher sun, one might expect a larger slope in relation (1) and

larger *DN* values of the target. Therefore, when smoothing is applied the slopes of the SPOT images could be slightly overcorrected compared with the Landsat images. Also, some differences in the spectral bands of Landsat and SPOT could cause systematic differences in reflectance for the same targets. It is well possible that the time series of SPOT images need a separate smoothing.

If possible, such vegetation types that have a minimum dependence of reflectance on the sun angle should be preferred for smoothing purposes. So, in part, the reflectance time courses obtained from such image series are formed by the change of the sun angle during the season. For a better comparative analysis of the time series and to amplify the phenology-related changes, the sun angle effects should somehow be eliminated. In part, this could be done by means of theoretical simulation. First of all, the sun angle effects should be studied by measurements as well as by theoretical simulation.

CONCLUSIONS

The seasonal course of reflectance as a function of temperature time was determined for several forest types in south-east Estonia from a set of Landsat TM and SPOT images. The obtained seasonal series are now suitable for interpretation. Our next efforts will be directed towards a systematic quantitative interpretation of the smoothed seasonal reflectance curves by means of model simulation and evaluation of the quantitative role of all driving factors in forming the seasonal changes. For instance, from the smoothed seasonal changes of reflectance it can easily be seen that the reflectance courses of fertile and infertile birch are different. So, there should be different driving factors, like the drying of ground surface during early spring and the time lag in green development for infertile birch stands when compared with the fertile birch.

The smoothed series of images could be used for analysing seasonal reflectance changes among other types of vegetation as well. A possible application in our case could be studying different types of wetland vegetation adjacent to the studied forest area. As an example, in the smoothed seasonal series, the influence of excess of water is clearly seen in the lowland mire site type, the seasonal reflectance curves being of different shape in wet and dry years. The seasonal course of the sun angle has to be taken into account to correctly interpret the time series.

After smoothing, the variability of seasonal series of reflectance among individual stands could still be quite high because of uncertainties introduced by the image rectification and the influence of boundary pixels. The larger the stand, the smaller should the variability be. A rough practical estimate obtained from this study is that a stand should be at least 5 ha in area to guarantee a more or less smooth seasonal behaviour of reflectance.

The smoothed seasonal curves could be used to reduce the seasonal effects in change detection and to study the primary productivity of different forest types by applying the Monteith hypothesis.

ACKNOWLEDGEMENTS

A considerable amount of satellite images of the time series were purchased within the framework of the VALERI project (INRA, Avignon, France). The kind help of the Estonian Meteorological and Hydrological Institute with the daily temperature and water level data is acknowledged. This work was supported by the Estonian Science Foundation grants Nos 6815 and 6100.

REFERENCES

Kuusk, A. & Nilson, T. 2000. A directional multispectral forest reflectance model. *Remote Sens. Environ*., **72**, 244–252.

Lükk, T. 1999. Satelliidipiltide heleduste arvutamine PixelWin programmiga. *Trans. Fac. For. Est. Agricult. Univ.*, No. 22, 88–95.

Monteith, J. L. 1972. Solar radiation and productivity in tropical ecosystems. *J. Appl. Ecol.*, **9**, 747–766.

Nilson, T. 1988. Spectral-temporal reflectance profiles for some cereals. *Estonian Acad. Sci. Preprint*, A-10.

Nilson, T., Kuusk, A., Lang, M. & Lükk, T. 2003. Forest reflectance modeling: theoretical aspects and applications. *Ambio*, **32**(8), 535–541.

Orlov, M. M. 1929. *Forest Taxation*. Leningrad (in Russian).

Peterson, U. 1992. Seasonal reflectance factor dynamics in boreal forest clear-cut communities. *Int. J. Remote Sens*., **13**(4), 753–772.

Vermote, E. F., Tanré, D., Deuzé, J. L., Herman, M. & Morcrette, J. J. 1997. Second simulation of the satellite signal in the solar spectrum, 6S: an overview. *IEEE Trans. Geosci. Remote Sens.*, **35**, 675–686.

Satelliidipiltide aegrea kaliibrimisest metsade heleduse sesoonse käigu uurimiseks

Tiit Nilson, Tõnu Lükk, Sandra Suviste, Heidi Kadarik ja Alo Eenmäe

Ajavahemikul 1986–2003 salvestatud Järvselja piirkonna Landsati TM-i ja SPOT-i satelliidipiltidest moodustati aegrida, et uurida erinevate metsatüüpide heleduskordajate sesoonset muutumist. Satelliidipildid teisendati maapinnalähedase heleduskordaja ühikutesse kõigis kuues Landsati TM-i lühilainelises spektraalkanalis. Erinevad metsatüübid valiti välja Järvselja majandi metsandusliku andmebaasi alusel. Sesoonne muutlikkus esitati fenoloogilise aja teljestikus. Piltide kaliibrimiskordajaid korrigeeriti nii, et saada siledad sesoonsed heleduskordaja käigud viljaka kasvukoha kuusikutele, männikutele ja kaasikutele kui tumedatele ja rabamännikutele kui heledatele objektidele. Tulemusena saadud silutud sesoonsed käigud on nüüd sobivad erinevate metsatüüpide heleduskordajate sesoonse muutumise seaduspärasuste kvantitatiivseks analüüsiks ja peamiste mõjufaktorite väljaselgitamiseks.